Dynamics of the cell-free DNA methylome of metastatic prostate cancer during androgen-targeting treatment

Running Head: cfDNA methylome in advanced prostate cancer

Authors: Madonna R. Peter[1,2], Misha Bilenky[3], Ruth Isserlin[4], Gary D. Bader[4], Shu Yi Shen[5], Daniel D. De Carvalho[5,6], Aaron R. Hansen[7], Pingzhao Hu[8], Neil E. Fleshner[9], Anthony M. Joshua[7,10], Martin Hirst[3,11], Bharati Bapat[1,2]*

Affiliations:

1. Lunenfeld-Tanenbaum Research Institute, Sinai Health System, Toronto, Canada.
2. Department of Laboratory Medicine & Pathobiology, University of Toronto, Toronto, Canada.
3. Canada's Michael Smith Genome Science Center, BC Cancer Agency, Vancouver, Canada.
4. Terrence Donnelly Centre for Cellular and Biomolecular Research, University of Toronto, Toronto, Canada.
5. Princess Margaret Cancer Centre, University Health Network, Toronto, Canada
6. Department of Medical Biophysics, University of Toronto. Toronto, Ontario, Canada
7. Division of Medical Oncology and Hematology, Princess Margaret Cancer Centre, Toronto, Canada.
8. Department of Biochemistry and Medical Genetics, University of Manitoba, Winnipeg, Canada.
9. Departments of Surgery and Surgical Oncology, Division of Urology, University Health Network, Toronto, Canada.
10. Department of Medical Oncology, Kinghorn Cancer Centre, Australia.
11. Department of Microbiology and Immunology and Michael Smith Laboratories, University of British Columbia, Vancouver, Canada.

*Corresponding author: Dr. Bharati Bapat. 60 Murray Street, Toronto, ON, Canada, M1B 1Y5. Telephone: 416-586-4800, Ext: 5175. Email: bapat@lunenfeld.ca

Abstract

Aim: We examined methylation changes in cell-free DNA (cfDNA) in metastatic castration resistant prostate cancer (mCRPC) during treatment. **Materials and Methods:** Genome-wide methylation analysis of sequentially collected cfDNA samples derived from mCRPC patients undergoing androgen-targeting therapy was performed. **Results:** Alterations in methylation states previously implicated in prostate cancer progression were observed and patients that maintained methylation changes throughout therapy tended to have a longer time to clinical progression (TTP). Importantly, we also report that markers associated with a highly aggressive form of the disease, Neuroendocrine-CRPC, were associated with a faster TTP. **Conclusion:** Our findings highlight the potential of monitoring cfDNA methylome during therapy in mCRPC, which may serve as predictive markers of response to androgen-targeting agents.

Key words: metastatic castration resistant prostate cancer, circulating cell free DNA, DNA methylation, epigenetic modifications, genome-wide methylation analysis

45 **Introduction**:

46 Prostate cancer (PCa) is the most common cancer and the second leading cause of cancer-
47 related deaths among males (1, 2). Androgen deprivation therapy (ADT) to reduce systemic
48 androgen levels continues to be the major treatment for aggressive PCa (3). While ADT is
49 initially beneficial, treatment resistance leads to the most lethal form of PCa, metastatic
50 castration resistant prostate cancer (mCRPC) (4). Despite castrate levels of systemic androgens,
51 these tumors can continue to rely on the androgen receptor (AR) pathway to promote tumor
52 growth and metastasis (5). Indeed, androgen-targeting agents, Enzalutamide and Abiraterone
53 acetate, can improve overall and progression-free survival in both the pre- and post-
54 chemotherapy settings (6-9).

55

56 Enzalutamide is an antiandrogen that directly inhibits full-length AR. Abiraterone
57 inhibits CYP17A1, which catalyzes extragonadal androgen production (10, 11). Both treatments
58 perform similarly to suppress the androgen pathway, and choice of treatment is often dependent
59 on comorbidities (12). However, primary and eventual secondary resistance to Abiraterone or
60 Enzalutamide remains an ongoing challenge. As a result, the treatment landscape of mCRPC is
61 complex and continues to focus primarily on the order/sequencing of therapies. For instance,
62 recent trials demonstrated early treatment with Abiraterone or Enzalutamide in the hormone-
63 sensitive state could be beneficial (13-15). However, there is a diverse array of molecular drivers
64 contributing to disease heterogeneity amongst mCRPC patients (16, 17), leading to variable
65 response to current treatment strategies. Therefore, reliable biomarkers are needed to facilitate
66 optimal therapy sequences for each patient prior to starting treatments.

67

68 Liquid biopsies are emerging as a minimally invasive source of biomarkers, reflecting
69 tumor turnover (18). Numerous studies have explored the potential of circulating tumor cell
70 (CTC) or circulating nucleic acid markers in mCRPC (19). Counting the number of CTCs and/or
71 characterization of molecular alterations (i.e. genomic and transcriptomic) are promising markers
72 that capture tumor heterogeneity (20). For instance, increased CTC number is associated with
73 poor prognosis, and expression of the ligand-independent AR-V7 splice variant by CTCs is
74 associated with resistance to Enzalutamide and Abiraterone (21-23). However, low CTC counts
75 prior to first-line treatment and the need for robust CTC surface markers for their optimal
76 detection remain an ongoing challenge (24, 25). Furthermore, some AR-V7 positive patients may
77 still benefit from androgen therapies, while certain AR-V7 negative patients show variability in
78 treatment response (26, 27). In addition, highly aggressive androgen-independent
79 Neuroendocrine-CRPC (NE-CRPC) tumors express lower levels of AR-V7 than
80 Adenocarcinoma-CRPC patients (28). Therefore, additional markers are needed to identify this
81 subset of patients.
82
83 Circulating cell free DNA (cfDNA) can harbor tumor-specific somatic mutations and
84 capture tumor heterogeneity (29). There is a high concordance (>90%) of tumor mutations (i.e.
85 *AR, BRCA2*) between matched cfDNA and mCRPC biopsies (18). Although the proportion of
86 circulating tumor DNA (ctDNA) can vary from 1-2% to ~30% of cfDNA in mCRPC, the
87 sequencing throughput of massively parallel sequencing platforms can sample cfDNA with
88 sufficient coverage (30). For instance, targeted sequencing of *AR* in cfDNA can detect mutations
89 associated with resistance to Enzalutamide or Abiraterone (31, 32). However, genomic
90 aberrations are not the only contributors to molecular and phenotypic heterogeneity in mCRPC.

91 Aberrations in the epigenome are a hallmark of all stages of PCa, including DNA methylation
92 alterations (33, 34). Hypermethylation in promoter regions of several genes, such as *GSTP1*,
93 *APC*, *HOXD3* and *TBX15*, are currently being investigated as diagnostic and prognostic markers
94 in earlier stages of PCa (34, 35). Furthermore, in biopsy tissue from metastatic lesions, distinct
95 DNA methylation patterns were observed between NE-CRPC and Adenocarcinoma-CRPC (28).
96
97 CpG methylation can be detected from DNA extracted from tissue and various biofluids
98 (36-38). Presence of promoter methylation in *GSTP1* and *APC* in cfDNA from mCRPC patients
99 is prognostic of overall survival (36, 39). Using an array-based platform, differential cfDNA
100 methylation patterns were observed between Abiraterone responsive versus resistant patients
101 (37). Recently, NE-CRPC tissue-derived methylation signals were shown to be detectable in
102 matched plasma samples (40). While these observations are promising, extensive genome wide
103 analysis of the mCRPC cfDNA methylome during Enzalutamide or Abiraterone treatment has
104 not been performed. To identify circulating DNA methylation changes associated with response
105 to either Enzalutamide or Abiraterone treatment, we monitored sequentially collected cfDNA
106 samples from mCRPC patients, starting from prior to treatment initiation to eventual clinical
107 progression, and performed genome-wide methylome assessment.
108
109 Given that biopsy tissue samples are not easily obtainable in the clinical setting,
110 especially bone metastases, we addressed whether analysis of intra-patient cfDNA methylation
111 changes without a priori knowledge of matched tumour methylation patterns, and/or integration
112 with tissue methylation datasets is required to correlate with response to treatment. We identified
113 key genes known to have altered methylation states in PCa and found genomic regions

114 associated with clinical progression. Furthermore, as these changes could be from tumour and
115 non-tumour derived cfDNA, we combined our findings with published data and revealed cfDNA
116 methylation patterns associated with worse clinical prognosis during androgen-targeting
117 treatment.
118

119 **Patients and Methods**

120 **Patient cohort**

121 All patients in this study were recruited from the Princess Margaret Cancer Centre
122 Genitourinary Clinic, and informed written consent was obtained in accordance with approved
123 institutional Research Ethics Board protocols from University Health Network (UHN) and Sinai
124 Health System (SHS). The UHN Genitourinary Biobank performed patient recruitment, blood
125 collection and clinical follow-up. All patients were chemotherapy naïve and developed resistance
126 following initial PCa treatments (local therapies and ADT) (**Supplementary Table 1**). A total of
127 12 Enzalutamide-treated (160 mg daily) and 4 Abiraterone-treated patients (1000 mg daily +
128 Prednisone/Dexamethasone) completed study visits for cfDNA methylome analysis. Blood was
129 collected at three time points: prior to starting treatment (**Visit A**), at 12-weeks during treatment
130 (**Visit B**) and upon clinical progression/treatment change (**Visit C**). While we aimed to collect
131 Visit B around week-12 (+/- 2 weeks), average time from baseline for Visit B was 12.7 weeks
132 (ranging 9 - 17 weeks). Serum PSA levels were obtained throughout treatment, and the lowest
133 PSA level (nadir) was used to determine PSA progression. Clinical progression was determined
134 by several factors, including radiological evidence of additional/worsening metastases and
135 symptomatic changes as assessed by the treating physician.
136

137 **Blood sample processing and cfDNA isolation**

138 Blood was collected at each time point in citrate cell preparation tubes (BD Biosciences,
139 San Jose, CA, USA) and samples were processed within 2 hours from collection. Plasma was
140 separated from peripheral blood mononuclear cells (PBMCs) by centrifugation at 1800 x g for 20
141 minutes. Isolated plasma was divided into 1 mL aliquots and stored at -80°C. Prior to cfDNA
142 isolation, frozen plasma samples were rapidly thawed at 37°C and spun at 16 000 x g for 5
143 minutes. For each visit, we utilized 4 mL of plasma and cfDNA was isolated using the QIAamp
144 Circulating Nucleic Acid Kit (Qiagen, Hilden, Germany). The concentration of cfDNA was
145 determined using the Qubit dsDNA High Sensitivity Assay Kit (ThermoFisher Scientific,
146 Waltham, MA, USA) and cfDNA fragment distibrution for subset of samples was obtained using
147 the Agilent 2100 Bioanalyzer System. To avoid within-patient batch effects, we isolated plasma
148 cfDNA and performed methylation analysis for all visits from each patient together.

149

150 **cfMeDIP-seq protocol**

151 Genome-wide methylation profiling was performed using a published protocol, cell-free
152 methylated DNA immunoprecipitation and high-throughput sequencing (cfMeDIP-seq) (41).
153 Briefly, isolated cfDNA was first end-repaired and A-tailed using the KAPA HyperPrep kit
154 (Roche, Mannheim, Germany), followed by adapter ligation with index adapters (Integrated
155 DNA technologies). Each adapter-ligated cfDNA sample was then spiked with λ phage DNA
156 (ThermoFisher Scientific) as filler DNA, as well as methylated and unmethylated control
157 *Arabidopsis thaliana* (AT) DNA (Diagenode, Denville, NJ, USA) to bring the total DNA amount
158 to 100ng. Prior to immunoprecipitation, 10% of this DNA is saved as input control. The
159 Diagenode MagMeDIP and IPure v2 kits were utilized to enrich and purify methylated cfDNA.

160 Prior to library amplification, qPCR quality checks were performed to ensure: (1) high
161 specificity (>95%) for enrichment of methylated AT DNA over unmethylated AT DNA, and (2)
162 appropriate adapter-ligation. This was followed by adapter-specific amplification of each MeDIP
163 and input control library and gel size selection. All sequencing was performed on the Illumina
164 HiSeq 2500 platform (50-bp single end reads).
165
166 **Sequencing data pre-processing and differential methylation analysis**
167 Raw sequencing data was aligned to hg19 reference genome using Burrows-Wheeler
168 alignment (BWA version 0.7.6a, using 'mem' option with default settings, except using –M
169 flag). Duplicated reads were marked by Picard tools (https://broadinstitute.github.io/picard/) and
170 collapsed to allow only one copy of the reads from reads that have the same alignment position.
171 Reads mapped to the multiple locations were removed by applying alignment quality threshold
172 (QA>5). As the sequencing data was single-end, the average DNA fragment length was
173 evaluated for both cfMeDIP and input controls using self-correlation technique (42). For each
174 library, the fragment coverage genomic profile was calculated using directional extension of all
175 aligned reads with estimated average fragment length (175bp in our case) using an in-house
176 BAM2WIG custom tool (M. Bilenky, unpublished, see http://www.epigenomes.ca/tools-and-
177 software). Within-patient differential methylation analysis for all comparisons was performed
178 using DMRHunter pipeline developed for cfDNA samples (**Supplemental Methods Section**).
179
180 **Statistical analysis of mCRPC-associated DMRs**
181 Spearman correlation analysis was performed using the base package of R (v3.5.3).
182 Receiver operating characteristic (ROC) curve analysis was performed using the pROC package

183 (1.14.0). All data was visualized using the ggplots2 package (v 3.1) and heatmaps from the
184 package ComplexHeatmap (1.2). Pathway analysis is described in **Supplemental Methods**
185 **Section**.
186
187 **Results:**
188 **Study design and patient cohort**
189 Tumor methylation signatures can be identified through comparison of cancer patients'
190 cfDNA with either matched tumor tissue or healthy control cfDNA (41). In the case of mCRPC,
191 biopsy of metastatic lesions in bone is not routinely feasible. Therefore, to identify methylation
192 markers associated with response to therapy, we opted for within/intra-patient differential
193 methylation analysis. We hypothesized that sequential collection of cfDNA from visit A
194 (baseline/pre-treatment) to visit B (week-12) to visit C (clinical progression) would reveal
195 changes in the cfDNA methylome that reflect responses to treatment, with each patient serving
196 as their own internal control. As outlined in **Figure 1**, intra-patient comparison could potentially
197 detect changes in abundance of methylated DNA fragments related to tumor response. For
198 instance, loss of methylated fragments may reflect loss/reduction of tumor cells sensitive to
199 treatment. In contrast, gains in methylated fragments could be associated with gains in treatment
200 resistant tumor cells, since changes in methylome could occur due to non-tumor/treatment
201 related changes. Therefore, we first examined intra-patient differentially methylated regions
202 (**DMRs**) to assess overall changes in cfDNA during treatment. We then integrated these DMRs
203 with tumour-derived methylation datasets.
204

205 We prospectively collected plasma from mCRPC patients receiving either Enzalutamide
206 (n=12) or Abiraterone acetate (n=4) treatment. In total, 45 blood samples were collected and
207 summarized in **Figure 2a**. Two Enzalutamide-treated patients were unable to provide Visit C
208 samples (P2 and P26) and one Abiraterone-treated patient progressed prior to Visit B (P36). The
209 majority of patients (14/16) presented with bone metastatic lesions upon mCRPC diagnosis, with
210 a subset showing lymph node and soft tissue metastases (**Figure 2b**). Twelve patients
211 demonstrated an initial favorable prostate-specific antigen (PSA) response (≥ 50% decline from
212 baseline, **Figure 2c**), and most patients exhibited maximal PSA response (favorable or plateau)
213 around Visit B (**Supplementary Figure 1**). Overall time to clinical progression (**TTP**) varied for
214 each patient, ranging from rapid/primary resistance to therapy to treatment-driven resistance
215 following initial favorable response (**Figure 2d**).
216
217 **Performance of cfMeDIP-seq strategy with PCa cell line DNA and cfDNA samples**
218 We utilized an established cfMeDIP-seq approach, which was developed for low amounts
219 of cfDNA and capable of ctDNA fractions as low as 0.001% (41). This technique was able to
220 distinguish methylation patterns between various cancer types, including pancreatic, breast and
221 colorectal cancer. Briefly, methylated cfDNA is enriched using an antibody specific for
222 methylated CpG sites, followed by amplification of adapter-ligated libraries. For each sample,
223 10% of the DNA was reserved as an input control (without immunoprecipitation).
224
225 To benchmark this methodology for PCa samples, we generated a control from genomic
226 DNA derived from PCa cell line, 22Rv1, sheared to the same size as cfDNA (**Supplementary**
227 **Figure 2**). As an additional control, we spiked all samples with methylated and unmethylated

228 *Arabidopsis thaliana* (AT) DNA, and confirmed increased recovery of methylated AT DNA
229 (~80%) compared to unmethylated DNA (<0.06%) (**Supplementary Figure 2a**). Spiked AT
230 DNA was added following sequencing adapter ligation to cfDNA and not detectable during
231 sequencing. Increased enrichment of known methylated genes/regions in the genome of 22Rv1
232 cells, (43) including the *CDKN2A* gene body and the first exon of *TGFB2,* compared to the
233 unmethylated promoter of *HOXD8* was confirmed (**Supplementary Figure 2b**).
234
235 We performed cfMeDIP-seq on all 45 samples collected. The average starting amount of
236 dsDNA was 27 ng, and ranged from 9 to 50 ng, with no significant differences in cfDNA
237 amounts across visits and treatments (**Supplementary Figure 2c**). Following alignment and base
238 quality filtering, 48-62% of the cfMeDIP reads and 80-85% of input control reads remained for
239 DMR analysis (**Supplementary Figure 2d-e**). A majority of cfMeDIP-seq sequence reads
240 aligned within gene bodies (major transcript starting from transcriptional start site/TSS to
241 transcription termination site/TTS) and intergenic regions, as well as CpG Island (CGI), CGI
242 shores, and TSS/promoter regions (TSS +/-1.5Kb), together representing the entire genome
243 (**Supplementary Figure 2f**). As expected, enrichment of methylated cfDNA in the MeDIP
244 fraction over input control fraction was observed, especially within CpG rich regions. Similar
245 distribution of regions was observed between Enzalutamide and Abiraterone treated patients
246 (**Supplementary Figure 2 g-h**).
247
248 **Intra-patient differential methylation analysis**
249 To identify treatment-related differentially methylated regions (DMRs), we developed a
250 DMR calling strategy for intra-patient analysis termed "cfDNA DMRHunter" (See

251 **Supplemental methods** and **Supplementary Figure 3**). As location-specific cfDNA recovery
252 sensitivity is unknown *a priori*, we used input control libraries to ensure uniform cfDNA read
253 coverage across the whole genome. DMRHunter also uses the input controls to remove
254 alignment artifacts from analysis. After filtering low quality and PCR duplicated reads,
255 DMRHunter builds a background model and identifies differentially methylated CpGs (DMCs)
256 across the genome. Adjacent DMCs with the same differential methylation state (UP or DOWN)
257 were merged to identify DMRs with stringent z-score (>1.5), average read count (≥10) and false
258 discovery rate (FDR = 0.01) cut-offs. There were a large number of DMRs across all
259 comparisons and treatments, ranging from 93 000 to 154 000 DMRs (**Figure 3a**) with no
260 significant difference in median number of DMRs between comparisons and treatment (**Figure**
261 **3b-c**). The overall median DMR size was 74 bp, ranging from 2bp (single CpG sites) up to 4163
262 bp.
263
264 We next examined the directionality of these changes across comparisons.
265 Conventionally, hypermethylation or hypomethylation is the typical terminology for methylation
266 changes. However, for cfDNA, it is unclear whether these changes reflect a gain/loss of
267 methylated CpGs at these specific genomic sites or changes in DNA fragment abundance,
268 reflecting an altered cellular abundance contributing to the cfDNA pool. For our analysis we
269 opted to define these DMRs as gains (UP) or loss (DOWN) in methylated fragments. There was
270 no significant difference in the overall proportion of regions with increased or decreased
271 methylation in all visit comparisons (**Figures 3d-f**). The majority of DMRs were found within
272 gene bodies (protein coding and pseudogenes) and intergenic regions (**Figure 3g**). DMRs
273 near/within transcription start sites (TSS)/promoters and CpG Islands (CGI), as well as non-

274 coding RNA (ncRNA), were found, but with lower abundance. We chose to focus on DMRs
275 within promoter and gene body regions, as CpG methylation changes in these locations are
276 known to be associated with gene expression changes (44).
277
278 **Methylation changes within promoter and gene body regions**
279 The majority of DMRs within promoters (TSS +/- 1.5 Kb) were associated with protein
280 coding (PC) genes, followed by long non-coding RNA (lncRNA), pseudogenes (Pseudo) and
281 short non-coding RNA (sncRNA) regions (**Supplementary Figure 4a**). We observed minimal
282 overlap among promoters of different gene/ncRNA categories, and overall distribution of DMRs
283 in these regions did not vary between patients and visits (**Supplementary Figure 4b**). We
284 focused on protein coding genes with at least one promoter DMR. Analyzing recurrence of these
285 genes, we found that many of these genes were found in less than 5 patients for each comparison
286 (**Supplementary Figure 4c-e**). We examined the most common protein coding genes (with
287 DMRs in ≥ 5 patients) and found many genes overlapping across visit comparisons, with the
288 majority shared between Abiraterone and Enzalutamide groups (**Figure 3h**). The most common
289 genes showing either increases or decreases in promoter methylation are in **Supplementary**
290 **Figure 4f**, with certain genes implicated in PCa or other cancers. For instance, pyrroline-5-
291 carboxylate reductase 1 (*PYCR1*), which is involved in proline biosynthesis and can promote
292 tumor cell growth (45), often demonstrated gain of methylation at visit C. Pathway enrichment
293 analysis of promoter DMRs (**Supplementary Figures 5 and 6**) showed cancer-related pathways
294 such as Wnt and PI3K signaling were observed, with neuronal pathways being the most frequent.
295 Several promoter associated DMRs were only found among Enzalutamide-treated patients
296 (**Figure 3h and Supplementary table 2)**. The most frequently differentially methylated

297 promoter region (6-7 patients, 20 comparisons) within the Enzalutamide cohort was *FGFR1*,
298 which is overexpressed in PCa and implicated in metastasis (46).
299
300 We also examined the distribution of DMRs within gene bodies/known transcripts. The
301 majority of these DMRs were associated with protein coding gene bodies across
302 (**Supplementary Figure 7a-b**). In contrast to promoter DMRs, many genes with body DMRs
303 were shared across patients (**Supplementary Figure 7c-e**). Similarly, we focused on commonly
304 altered gene bodies and found extensive overlap between visit comparisons and treatments
305 (**Figure 3i**). We further examined net methylation change across these genes by scoring the ratio
306 of increased to decreased methylation within each gene body, excluding genes that had no net
307 change (i.e. equal number of UP and DOWN trends). We found 91 genes that were commonly
308 altered across all comparisons (**Supplementary Figure 7f**). In most cases, regardless of visit
309 comparison, the methylation pattern for these genes clustered closely for the same patients. One
310 such group of genes with increases in methylation at Visit C included *NFATC1*, which can
311 promote tumorigenesis (47), and a histone deacetylase, *HDAC4*. While several Enzalutamide-
312 specific genes were found (**Supplementary table 3**), common pathways including several
313 differentiation-related and neuronal pathways were found among gene-body associated DMRs
314 (**Supplementary Figures 8 & 9**).
315
316 Overall, examining the most frequently altered promoters or gene bodies revealed a few
317 cancer-related genes, but changes across all visit comparisons were variable. We assessed the
318 overall promoter methylation status of genes that have been established as differentially
319 methylated in PCa (**Figure 4a**), including *GSTP1*, *TBX15*, *AOX1* and members of the HOX

320 family of transcription factors (34). Among the most common differentially methylated gene
321 promoters were genes involved in tumorigenic processes, such as *RUNX3*, *RGS12* and *FBP1*,
322 with several differentially expressed in NE-CRPC (28), including the neuronal transcription
323 factor *PHOX2A* (48) and a regulator of apoptosis, *CTBP2* (49). DMRs in genes associated with
324 diagnosis and prognosis could reflect tumor cell response to treatments. While differential
325 promoter methylation events in the well-established PCa-specific hypermethylated gene, *GSTP1*,
326 were infrequent (**Figure 4b**), decreased gene body methylation coinciding with treatment
327 response (i.e. PSA reduction) was shown in some patients (i.e. P3). Similar methylation regions
328 were also observed in the PCa cell line LNCaP (50). Similarly, changes in *TBX15* methylation
329 (1st intron) were associated with response to treatment (i.e. PSA) in certain patients (**Figure 4c**).
330 While promising, there were no consistent DMRs in these genes that could classify patients by
331 androgen-targeting treatment response. To further refine potential treatment associated
332 methylation changes, locations within the genome that experienced fluctuations in methylation
333 levels across all visits were next explored.
334
335 **Common CpG sites with differential methylation across treatment visits**
336 To find potential "treatment sensitive" CpG sites in the genome, we next examined
337 differentially methylated CpG sites (DMCs) among patients that completed all study visits,
338 specifically CpG sites that fluctuated in ≥2 visit comparisons. DMCs were analyzed as DMR size
339 for similar genomic regions varied within and across patients. We stratified the proportion of
340 DMCs that were uniquely found in single visit comparisons and those shared across all visits
341 (Scenarios 1-6 in **Figure 5a**). We identified DMCs present in two or more visit comparisons for
342 each patient (Scenarios 7-14) and associated them with gene promoters and bodies. Analysis of

343 gene promoters containing DMCs revealed minimal overlap amongst patients, with P4, P31, P38
344 and P3 showing the highest overlap of 8 shared genes: *NPBWR1*, *ZSCAN12*, *PCDHGA11*,
345 *PHOX2A*, *TBX10*, *TEX28*, *TKTL1* and *TSPAN32* (**Supplementary Figure 10a**). In contrast, we
346 observed a high degree of overlap amongst patients when looking at DMCs within gene bodies,
347 with the exception of P3 (**Supplementary Figure 10b**). Interestingly, we also noted a positive
348 correlation between the proportion of DMCs shared across all visits and TTP (**Figure 5a**).
349
350 We examined 3 major combined scenarios observed among 14 total: (1)
351 increase/decrease in methylation in visit C vs B and A (scenarios 7 and 8) (**Figure 5a**); (2)
352 increase/decrease in B and C vs A (scenarios 9 and 10,); (3) those that increase /decrease in B vs
353 A and then return to same levels in C (13 &14). The proportion of these three combined
354 scenarios was correlated with time to progression (TTP), and we found that those patients with
355 more DMCs that increased/decreased at visit B and maintained at visit C (scenarios 9 and 10)
356 had a longer TTP (**Figure 5b**). Although scenarios 7 & 8 did not correlate with TTP, those
357 patients with a higher proportion of scenarios 13 & 14 had a possible trend towards faster TTP
358 (**Supplementary figure 10 c-d**, p=0.05). This suggests that genome-wide cfDNA methylation
359 dynamics can reflect response to treatment in mCRPC patients. Importantly, changes in
360 methylation levels of these specific regions/genes could potentially be used as a monitoring tool
361 during androgen-target treatment.
362
363 **Neuroendocrine-CRPC related cfDNA DMRs**
364 Thus far, fluctuations in DMRs were analyzed for all cfDNA signals, which could include
365 tumour and non-tumour derived DNA. As many of the DMRs were associated with genes

366 implicated in several neuronal pathways and differentiation, we integrated cfDNA DMRs with
367 those identified from biopsy samples from NE-CRPC versus Adenocarcinoma-CRPC in an
368 independent mCRPC patient series (28). While this published dataset utilized reduced
369 representation bisulfite sequencing (RRBS), which primarily covers CpG rich regions (i.e.
370 CGIs), several of these DMCs were found within cfDNA DMRs (29 355 CpG sites out of 84 930
371 in NE-CRPC). In order to assess whether changes in these regions at earlier time points are
372 associated with overall response to androgen-targeting agents, we examined the overlap between
373 DMRs from the A vs B comparison and NE-associated DMRs. As P36 progressed prior to visit
374 B (**Figure 2d**), we included this patient in the analysis (examining A vs C). In this case, we
375 examined the changes in methylation from the perspective of visit A. That is, increased
376 methylation in visit A vs B/C (UP in A) or decreased methylation in visit A (DOWN in A). We
377 proposed that the abundance of methylated cfDNA fragments from certain regions may reflect
378 key genes/regions to monitor prior to initiating therapy. The overall proportion of these DMRs
379 that were increased or decreased in methylation at A vs B (or C for ID 36) varied across the
380 patients (**Figure 6a**). Interestingly, we noted that these DMRs (A vs B) appeared to be related to
381 TTP. We examined the ratio of DMRs containing NE-CRPC associated CpG sites with more
382 methylated fragments in Visit A to those with less methylation. In order to further delineate key
383 regions, we applied various FDR thresholds to these DMRs to examine the effect on correlation
384 with TTP (**Figure 6b**). We found an optimal set of regions that were negatively correlated with
385 TTP: that is, the more methylated cfDNA fragments containing these NE-CRPC associated
386 CpGs, the faster/shorter the TTP (**Figure 6c**). In a follow-up study analyzing matched biopsy and
387 plasma methylation signals from 5 Adenocarcinoma-CRPC and 6 NE-CRPC patients, several
388 prostate cancer and Neuroendocrine related methylation regions were found in cfDNA (40). We

389 also integrated our A vs B DMRs with this dataset and found similar correlation with TTP
390 (Spearman R = -0.56, p = 0.024). To determine whether the amount of NE-CRPC related
391 methylation patterns at visit A was associated with a faster TTP, we performed ROC analysis for
392 various TTP cut-offs (ranging from ≤20 to 35 weeks). We found that an increased ratio of NE-
393 CRPC DMRs UP in visit A can stratify patients that progressed as early as 25-weeks (area under
394 the curve, AUC: 0.927, CI: 0.773-1) (**Figure 6d**). These findings confirm the detection of NE-
395 CRPC related methylation signatures in cfDNA, but also show for the first time that these sites
396 may serve as potential predictive markers of resistance to androgen-targeting agents.
397

398 **Discussion**

399 In this study, we showed that methylome analysis of the cfDNA from mCRPC patients
400 can capture treatment-related epigenetic alterations, with and without integration with tissue
401 derived methylation data. We found changes in well-established PCa methylation markers
402 associated with response to treatment. Importantly, we demonstrated that cfDNA contains NE-
403 CRPC related methylation signals, which have the potential to be utilized as predictive markers
404 of treatment response. Methylation of several oncogenic driving pathways were detected in
405 cfDNA across time points, suggesting that methylome analysis of patients' liquid biopsies can
406 serve as a monitoring tool during treatment, as well as highlight potential targets for future
407 therapies.
408

409 A key advantage of liquid biopsy-based versus tissue-biopsy approaches is the ability to
410 capture tumor heterogeneity. To date, much focus has been placed on genomic alterations, which
411 can help identify *AR* mutations related to resistance to Abiraterone/Enzalutamide (31, 32).

412 However, few studies have highlighted that cfDNA methylation markers may help further
413 stratify patients (36, 37). In a recent study of 600 mCRPC patients receiving docetaxel, increased
414 methylated *GSTP1* at baseline was associated with longer overall survival, and loss of
415 methylation after two cycles of treatment corresponded with longer time to PSA progression
416 (51). Furthermore, patients that exhibited loss in methylated *GSTP1* after two cycles of treatment
417 had better overall survival. In this study, we observed some cases in which there were losses of
418 *GSTP1* methylation in certain treatment responsive patients (PSA reduction). We also examined
419 other tissue-based methylation markers (promoter and gene body), including *TBX15* and *RUNX3*
420 (34), and similar heterogeneity amongst patients was observed. This in part could be explained
421 by differing mechanisms between docetaxel and androgen-targeting agents. Due to intra- and
422 inter-tumor heterogeneity (52, 53), androgen-targeting agents may not target all androgen-
423 independent tumor cells, which could also harbor these methylation markers. Furthermore, most
424 well-studied methylation markers were derived from earlier stages of PCa, whereas further
425 epigenomic instability is known to occur with the mCRPC state (54).
426
427 Through sequential analysis using a genome-wide approach, we highlighted progressive
428 changes in genes involved in tumorigenic processes in PCa and other cancers. Commonly altered
429 genes in the promoter region included *PYCR1* and *SHARPIN,* which are known to be upregulated
430 in PCa tissue and involved in processes such as proliferation and angiogenesis (55). Gene body
431 methylation changes were observed in genes that regulate various tumorigenic processes,
432 including *NFATC1* (47)*, PRDM16* (56), and *OPCML* (57). Pathway analysis also further
433 highlighted key mechanisms that have been established in prostate tumor tissue studies,

434 including the wnt pathway (16). However, the methylation patterns amongst these genes
435 demonstrated extensive variability across patients and visits.
436
437 In order to further delineate key regions, we further assessed common regions that
438 changed during treatment. These changes appeared to reflect dynamics of treatment response.
439 For instance, patients that demonstrated CpG changes (up or down) in visit B and sustained the
440 changes by visit C appeared to have a longer TTP. In contrast, there was a trend towards shorter
441 TTP amongst patients that did not demonstrate sustained methylation changes. Among the genes
442 included was Neuropeptides B/W receptor 1 (*NPBWR1*), which was shown to be upregulated in
443 basal cells from prostate tissue (58), thus highlighting that genome-wide cfDNA methylation
444 analysis is able to capture tumor dynamics and may further have additive potential to mutation
445 analysis.
446
447 We also observed that many of the differentially methylated genes overlapped between
448 Enzalutamide- and Abiraterone-treated patients. Although there are ongoing studies to compare
449 efficacy of either treatment (59), the current consensus is that both perform similarly, and
450 deciding between treatments in a patient-specific manner remains an ongoing challenge. We
451 identified sets of genes altered in the promoter and gene body locations, including one large set
452 amongst Enzalutamide treated patients. We were limited by the number of Abiraterone-treated
453 patients, which may have limited heterogeneity, as seen in the larger Enzalutamide cohort.
454 Further studies are needed to examine if the methylome is different between these treatment
455 types. However, similar pathways were observed between the treatments, with neuronal
456 pathways being the most prominent.

457

458 Given these neuronal-related genes/pathways, we wanted to examine the utility of these
459 methylation changes in helping to predict treatment outcome, especially in identifying
460 Neuroendocrine-CRPC. With our unique study design of sequential sampling, we could detect
461 these methylation trends at earlier time points, demonstrating that the proportion of
462 Neuroendocrine-like DMRs correlated with faster/shorter time to progression. In particular, the
463 higher the proportion of certain DMRs with these NE-CRPC associated methylation patterns, the
464 faster the time to progression. While we did not have confirmatory biopsies or other markers of
465 NE disease (i.e. chromogranin A), increased methylation at Visit A could be utilized as
466 predictive markers of response to androgen-targeting agents. Although we are currently limited
467 to a single cohort, we now have a set of candidate regions that could be validated in additional
468 cohorts.

469

470 **Conclusions**

471 Our genome-wide sequencing protocol and analysis strategy has demonstrated the utility
472 of intra-patient monitoring of cfDNA methylation. If changes in the methylome during treatment
473 were sustained until clinical progression, these patients appeared to have a better prognosis with
474 androgen-targeting treatment. Interestingly, methylation patterns associated with a highly
475 aggressive form of the disease may serve as potential predictive markers. Further independent
476 validation of these markers is needed to assess this predictive potential.

477

478

479

480 **Future Perspectives**

481 Liquid biopsy based biomarkers will be playing a major role in how we treat patients
482 with highly aggressive prostate cancer. Many studies focused primarily on genomic alterations
483 associated with treatment resistance, but epigenomic markers could further explain the molecular
484 heterogeneous mechanisms that contribute to disease progression. Ultimately, we anticipate that
485 a combination of genomic and epigenomic markers will help facilitate optimal therapy decisions.
486

487 **Summary points**

488 • We performed genome-wide methylation analysis of sequentially collected cfDNA
489 samples from mCRPC patients receiving androgen-targeting therapy
490 • The DMRHunter pipeline was developed to identify differentially methylation regions
491 between study visits for each patient
492 • Changes in promoter and gene body methylation was identified in key novel genes as
493 well as previously established genes associated with tumourigenesis and the highly
494 aggressive form of the disease, Neuroendocrine-CRPC
495 • Patients that were able to sustain methylation changes throughout treatment tended to
496 present a longer time to clinical progression, suggesting that fluctuations in these CpG
497 sites could help monitor response to treatment
498 • Elevated levels of Neuroendocrine-CRPC related methylation signals could serve
499 potential predictive markers of resistance to androgen
500 • These findings could help with improving the clinical management of mCRPC using a
501 minimally invasive approach
502

503 **Authors' contributions:** B.B. designed the study for intra-patient comparison. A.M.J. designed
504 the clinical study for patient recruitment and sample collection. P.H. provided sample size
505 calculations required for recruitment. M.R.P. performed sample processing, cfMeDIP-seq library
506 preparation, and data analysis. M.B. developed and executed the DMRHunter pipeline and along
507 with M.H., assisted with analysis to interpret cfMeDIP-seq datasets. R.I. and G.D.B. performed
508 pathway analysis. S.Y.S. and D.D.D.C. designed the cfMeDIP–seq protocol and assisted with
509 optimization for this study design. A.M.J., N.E.F. and A.R.H. were involved in patient follow-up
510 and interpretation of data in the context of clinicopathological parameters. M.R.P., M.B. and
511 B.B. composed the manuscript with feedback from all co-authors involved.
512
513 **Acknowledgements:** We acknowledge the UHN Genitourinary clinic and Genitourinary
514 Biobank for recruiting patients, collecting blood samples and for patient follow-up/data
515 collection. All sequencing and initial data pre-processing was performed by the Princess
516 Margaret Genomics Centre and the UHN Bioinformatics and HPC Core, Princess Margaret
517 Cancer Centre, respectively. Differential methylation analysis was performed using the facilities
518 provided by the Canada's Michael Smith Genome Sciences Centre (British Columbia Cancer
519 Agency). We also acknowledge Shivani Kamdar (SHS/LTRI) for assisting with sample
520 processing and for helping to edit this manuscript.
521
522 **Disclosures:** There are no financial or non-financial interests to be declared.
523
524 **Ethics approval and consent to participate:** All patients in this study provided informed
525 written consent in accordance with approved institutional Research Ethics Board protocols from

University Health Network (UHN) and Sinai Health System (SHS). Progress updates were submitted and approved annually by respective Research Ethics Boards. The study was performed in accordance with the Declaration of Helsinki. No personal information for any patient is presented in this manuscript. According to REB approvals, each patient was assigned unique study identifiers, which are not linked to personal health information.

Availability of data and materials: All FASTQ and QC files will be made available in a public repository upon publication of this manuscript. Additional supplementary data files have also been included.

Funding: This study was supported by a Prostate Cancer Canada Movember Discovery Grant (D2014-10) and an Astellas Prostate Cancer Innovation Fund (2017) to B. Bapat.

549 **References**

550 1. Bray F, Ferlay J, Soerjomataram I, Siegel RL, Torre LA, and Jemal A. Global cancer
551 statistics 2018: GLOBOCAN estimates of incidence and mortality worldwide for 36
552 cancers in 185 countries. *CA Cancer J Clin.* 68(6), 394-424 (2018).
553 2. Global Burden of Disease Cancer C, Fitzmaurice C, Allen C, Barber RM, Barregard L,
554 Bhutta ZA, et al. Global, Regional, and National Cancer Incidence, Mortality, Years of
555 Life Lost, Years Lived With Disability, and Disability-Adjusted Life-years for 32 Cancer
556 Groups, 1990 to 2015: A Systematic Analysis for the Global Burden of Disease Study.
557 *JAMA Oncology.* 3(4), 524-48 (2017).
558 3. Wong YN, Ferraldeschi R, Attard G, and de Bono J. Evolution of androgen receptor
559 targeted therapy for advanced prostate cancer. *Nat Rev Clin Oncol.* 11(6), 365-76 (2014).
560 4. Sridhar SS, Freedland SJ, Gleave ME, Higano C, Mulders P, Parker C, et al. Castration-
561 resistant prostate cancer: from new pathophysiology to new treatment. *Eur Urol.* 65(2),
562 289-99 (2014).
563 5. Crawford ED, Petrylak D, and Sartor O. Navigating the evolving therapeutic landscape in
564 advanced prostate cancer. *Urol Oncol.* 35S, S1-S13 (2017).
565 6. Scher HI, Fizazi K, Saad F, Taplin ME, Sternberg CN, Miller K, et al. Increased survival
566 with enzalutamide in prostate cancer after chemotherapy. *N Engl J Med.* 367(13), 1187-
567 97 (2012).
568 7. Loriot Y, Miller K, Sternberg CN, Fizazi K, De Bono JS, Chowdhury S, et al. Effect of
569 enzalutamide on health-related quality of life, pain, and skeletal-related events in
570 asymptomatic and minimally symptomatic, chemotherapy-naive patients with metastatic
571 castration-resistant prostate cancer (PREVAIL): results from a randomised, phase 3 trial.
572 *Lancet Oncol.* 16(5), 509-21 (2015).
573 8. de Bono JS, Logothetis CJ, Molina A, Fizazi K, North S, Chu L, et al. Abiraterone and
574 increased survival in metastatic prostate cancer. *N Engl J Med.* 364(21), 1995-2005
575 (2011).
576 9. Ryan CJ, Smith MR, Fizazi K, Saad F, Mulders PF, Sternberg CN, et al. Abiraterone
577 acetate plus prednisone versus placebo plus prednisone in chemotherapy-naive men with
578 metastatic castration-resistant prostate cancer (COU-AA-302): final overall survival
579 analysis of a randomised, double-blind, placebo-controlled phase 3 study. *Lancet Oncol.*
580 16(2), 152-60 (2015).
581 10. Bambury RM, and Scher HI. Enzalutamide: The story of its development from bench to
582 bedside. *Urol Oncol.* (2015).
583 11. Grist E, de Bono JS, and Attard G. Targeting extra-gonadal androgens in castration-
584 resistant prostate cancer. *J Steroid Biochem Mol Biol.* 145(157-63 (2015).
585 12. Sumanasuriya S, and De Bono J. Treatment of Advanced Prostate Cancer-A Review of
586 Current Therapies and Future Promise. *Cold Spring Harb Perspect Med.* 8(6), (2018).
587 13. Fizazi K, Tran N, Fein L, Matsubara N, Rodriguez-Antolin A, Alekseev BY, et al.
588 Abiraterone plus Prednisone in Metastatic, Castration-Sensitive Prostate Cancer. *N Engl J*
589 *Med.* 377(4), 352-60 (2017).
590 14. James ND, de Bono JS, Spears MR, Clarke NW, Mason MD, Dearnaley DP, et al.
591 Abiraterone for Prostate Cancer Not Previously Treated with Hormone Therapy. *N Engl J*
592 *Med.* 377(4), 338-51 (2017).

593 15. Armstrong AJ, Szmulewitz RZ, Petrylak DP, Holzbeierlein J, Villers A, Azad A, et al.
594 ARCHES: A Randomized, Phase III Study of Androgen Deprivation Therapy With
595 Enzalutamide or Placebo in Men With Metastatic Hormone-Sensitive Prostate Cancer. *J*
596 *Clin Oncol.* JCO1900799 (2019).
597 16. Robinson D, Van Allen EM, Wu YM, Schultz N, Lonigro RJ, Mosquera JM, et al.
598 Integrative clinical genomics of advanced prostate cancer. *Cell.* 161(5), 1215-28 (2015).
599 17. Armenia J, Wankowicz SAM, Liu D, Gao J, Kundra R, Reznik E, et al. The long tail of
600 oncogenic drivers in prostate cancer. *Nat Genet.* 50(5), 645-51 (2018).
601 18. Wyatt AW, Annala M, Aggarwal R, Beja K, Feng F, Youngren J, et al. Concordance of
602 Circulating Tumor DNA and Matched Metastatic Tissue Biopsy in Prostate Cancer. *J*
603 *Natl Cancer Inst.* 109(12), (2017).
604 19. Morrison GJ, and Goldkorn A. Development and Application of Liquid Biopsies in
605 Metastatic Prostate Cancer. *Curr Oncol Rep.* 20(4), 35 (2018).
606 20. Liu W, Yin B, Wang X, Yu P, Duan X, Liu C, et al. Circulating tumor cells in prostate
607 cancer: Precision diagnosis and therapy. *Oncol Lett.* 14(2), 1223-32 (2017).
608 21. Heller G, McCormack R, Kheoh T, Molina A, Smith MR, Dreicer R, et al. Circulating
609 Tumor Cell Number as a Response Measure of Prolonged Survival for Metastatic
610 Castration-Resistant Prostate Cancer: A Comparison With Prostate-Specific Antigen
611 Across Five Randomized Phase III Clinical Trials. *J Clin Oncol.* 36(6), 572-80 (2018).
612 22. Bastos DA, and Antonarakis ES. CTC-derived AR-V7 detection as a prognostic and
613 predictive biomarker in advanced prostate cancer. *Expert Rev Mol Diagn.* 18(2), 155-63
614 (2018).
615 23. Scher HI, Graf RP, Schreiber NA, Jayaram A, Winquist E, McLaughlin B, et al.
616 Assessment of the Validity of Nuclear-Localized Androgen Receptor Splice Variant 7 in
617 Circulating Tumor Cells as a Predictive Biomarker for Castration-Resistant Prostate
618 Cancer. *JAMA Oncol.* (2018).
619 24. Antonarakis ES, Lu C, Luber B, Wang H, Chen Y, Zhu Y, et al. Clinical Significance of
620 Androgen Receptor Splice Variant-7 mRNA Detection in Circulating Tumor Cells of
621 Men With Metastatic Castration-Resistant Prostate Cancer Treated With First- and
622 Second-Line Abiraterone and Enzalutamide. *J Clin Oncol.* 35(19), 2149-56 (2017).
623 25. Millner LM, Linder MW, and Valdes R, Jr. Circulating tumor cells: a review of present
624 methods and the need to identify heterogeneous phenotypes. *Ann Clin Lab Sci.* 43(3),
625 295-304 (2013).
626 26. Bernemann C, Schnoeller TJ, Luedeke M, Steinestel K, Boegemann M, Schrader AJ, et
627 al. Expression of AR-V7 in Circulating Tumour Cells Does Not Preclude Response to
628 Next Generation Androgen Deprivation Therapy in Patients with Castration Resistant
629 Prostate Cancer. *Eur Urol.* (2016).
630 27. Takeuchi T, Okuno Y, Hattori-Kato M, Zaitsu M, and Mikami K. Detection of AR-V7
631 mRNA in whole blood may not predict the effectiveness of novel endocrine drugs for
632 castration-resistant prostate cancer. *Res Rep Urol.* 8(21-5 (2016).
633 28. Beltran H, Prandi D, Mosquera JM, Benelli M, Puca L, Cyrta J, et al. Divergent clonal
634 evolution of castration-resistant neuroendocrine prostate cancer. *Nat Med.* 22(3), 298-305
635 (2016).
636 29. Corcoran RB, and Chabner BA. Application of Cell-free DNA Analysis to Cancer
637 Treatment. *N Engl J Med.* 379(18), 1754-65 (2018).

638 30. Ritch E, and Wyatt AW. Predicting therapy response and resistance in metastatic prostate
639 cancer with circulating tumor DNA. *Urol Oncol.* (2017).
640 31. Romanel A, Tandefelt DG, Conteduca V, Jayaram A, Casiraghi N, Wetterskog D, et al.
641 Plasma AR and abiraterone-resistant prostate cancer. *Sci Transl Med.* 7(312), 312re10
642 (2015).
643 32. Azad AA, Volik SV, Wyatt AW, Haegert A, Le Bihan S, Bell RH, et al. Androgen
644 Receptor Gene Aberrations in Circulating Cell-Free DNA: Biomarkers of Therapeutic
645 Resistance in Castration-Resistant Prostate Cancer. *Clin Cancer Res.* 21(10), 2315-24
646 (2015).
647 33. Yegnasubramanian S. Prostate cancer epigenetics and its clinical implications. *Asian*
648 *Journal of Andrology.* 18(4), 549-58 (2016).
649 34. Massie CE, Mills IG, and Lynch AG. The importance of DNA methylation in prostate
650 cancer development. *J Steroid Biochem Mol Biol.* 166(1-15 (2017).
651 35. Kron K, Liu L, Trudel D, Pethe V, Trachtenberg J, Fleshner N, et al. Correlation of ERG
652 expression and DNA methylation biomarkers with adverse clinicopathologic features of
653 prostate cancer. *Clin Cancer Res.* 18(10), 2896-904 (2012).
654 36. Mahon KL, Qu W, Devaney J, Paul C, Castillo L, Wykes RJ, et al. Methylated
655 Glutathione S-transferase 1 (mGSTP1) is a potential plasma free DNA epigenetic marker
656 of prognosis and response to chemotherapy in castrate-resistant prostate cancer. *Br J*
657 *Cancer.* 111(9), 1802-9 (2014).
658 37. Gordevicius J, Krisciunas A, Groot DE, Yip SM, Susic M, Kwan A, et al. Cell-Free DNA
659 Modification Dynamics in Abiraterone Acetate-Treated Prostate Cancer Patients. *Clin*
660 *Cancer Res.* 24(14), 3317-24 (2018).
661 38. Zhao F, Olkhov-Mitsel E, van der Kwast T, Sykes J, Zdravic D, Venkateswaran V, et al.
662 Urinary DNA Methylation Biomarkers for Noninvasive Prediction of Aggressive Disease
663 in Patients with Prostate Cancer on Active Surveillance. *J Urol.* 197(2), 335-41 (2017).
664 39. Hendriks RJ, Dijkstra S, Smit FP, Vandersmissen J, Van de Voorde H, Mulders PFA, et
665 al. Epigenetic markers in circulating cell-free DNA as prognostic markers for survival of
666 castration-resistant prostate cancer patients. *Prostate.* (2018).
667 40. Beltran H, Romanel A, Conteduca V, Casiraghi N, Sigouros M, Franceschini GM, et al.
668 Circulating tumor DNA profile recognizes transformation to castration-resistant
669 neuroendocrine prostate cancer. *J Clin Invest.* (2020).
670 41. Shen SY, Singhania R, Fehringer G, Chakravarthy A, Roehrl MHA, Chadwick D, et al.
671 Sensitive tumour detection and classification using plasma cell-free DNA methylomes.
672 *Nature.* 563(7732), 579-83 (2018).
673 42. Ramachandran P, Palidwor GA, Porter CJ, and Perkins TJ. MaSC: mappability-sensitive
674 cross-correlation for estimating mean fragment length of single-end short-read
675 sequencing data. *Bioinformatics.* 29(4), 444-50 (2013).
676 43. Kamdar SN, Ho LT, Kron KJ, Isserlin R, van der Kwast T, Zlotta AR, et al. Dynamic
677 interplay between locus-specific DNA methylation and hydroxymethylation regulates
678 distinct biological pathways in prostate carcinogenesis. *Clin Epigenetics.* 8(32 (2016).
679 44. Baylin SB, and Jones PA. Epigenetic Determinants of Cancer. *Cold Spring Harb*
680 *Perspect Biol.* 8(9), (2016).
681 45. Zeng T, Zhu L, Liao M, Zhuo W, Yang S, Wu W, et al. Knockdown of PYCR1 inhibits
682 cell proliferation and colony formation via cell cycle arrest and apoptosis in prostate
683 cancer. *Med Oncol.* 34(2), 27 (2017).

684 46. Yang F, Zhang Y, Ressler SJ, Ittmann MM, Ayala GE, Dang TD, et al. FGFR1 is
685 essential for prostate cancer progression and metastasis. *Cancer Res.* 73(12), 3716-24
686 (2013).
687 47. Manda KR, Tripathi P, Hsi AC, Ning J, Ruzinova MB, Liapis H, et al. NFATc1 promotes
688 prostate tumorigenesis and overcomes PTEN loss-induced senescence. *Oncogene.*
689 35(25), 3282-92 (2016).
690 48. Wang R, Chen X, Xu T, Xia R, Han L, Chen W, et al. MiR-326 regulates cell
691 proliferation and migration in lung cancer by targeting phox2a and is regulated by
692 HOTAIR. *Am J Cancer Res.* 6(2), 173-86 (2016).
693 49. Takayama K, Suzuki T, Fujimura T, Urano T, Takahashi S, Homma Y, et al. CtBP2
694 modulates the androgen receptor to promote prostate cancer progression. *Cancer Res.*
695 74(22), 6542-53 (2014).
696 50. Yang YA, Zhao JC, Fong KW, Kim J, Li S, Song C, et al. FOXA1 potentiates lineage-
697 specific enhancer activation through modulating TET1 expression and function. *Nucleic*
698 *Acids Res.* 44(17), 8153-64 (2016).
699 51. Mahon KL, Qu W, Lin HM, Spielman C, Cain D, Jacobs C, et al. Serum Free Methylated
700 Glutathione S-transferase 1 DNA Levels, Survival, and Response to Docetaxel in
701 Metastatic, Castration-resistant Prostate Cancer: Post Hoc Analyses of Data from a Phase
702 3 Trial. *Eur Urol.* (2018).
703 52. Brocks D, Assenov Y, Minner S, Bogatyrova O, Simon R, Koop C, et al. Intratumor
704 DNA methylation heterogeneity reflects clonal evolution in aggressive prostate cancer.
705 *Cell Reports.* 8(3), 798-806 (2014).
706 53. Aryee MJ, Liu W, Engelmann JC, Nuhn P, Gurel M, Haffner MC, et al. DNA
707 methylation alterations exhibit intraindividual stability and interindividual heterogeneity
708 in prostate cancer metastases. *Sci Transl Med.* 5(169), 169ra10 (2013).
709 54. Friedlander TW, Roy R, Tomlins SA, Ngo VT, Kobayashi Y, Azameera A, et al.
710 Common structural and epigenetic changes in the genome of castration-resistant prostate
711 cancer. *Cancer Res.* 72(3), 616-25 (2012).
712 55. Huang H, Du T, Zhang Y, Lai Y, Li K, Fan X, et al. Elevation of SHARPIN Protein
713 Levels in Prostate Adenocarcinomas Promotes Metastasis and Impairs Patient Survivals.
714 *Prostate.* 77(7), 718-28 (2017).
715 56. Zhu S, Xu Y, Song M, Chen G, Wang H, Zhao Y, et al. PRDM16 is associated with
716 evasion of apoptosis by prostatic cancer cells according to RNA interference screening.
717 *Mol Med Rep.* 14(4), 3357-61 (2016).
718 57. Simovic I, Castano-Rodriguez N, and Kaakoush NO. OPCML: A Promising Biomarker
719 and Therapeutic Avenue. *Trends Cancer.* 5(8), 463-6 (2019).
720 58. Zhang D, Park D, Zhong Y, Lu Y, Rycaj K, Gong S, et al. Stem cell and neurogenic
721 gene-expression profiles link prostate basal cells to aggressive prostate cancer. *Nat*
722 *Commun.* 7(10798 (2016).
723 59. Hara I, Yamashita S, Nishizawa S, Kikkawa K, Shimokawa T, and Kohjimoto Y.
724 Enzalutamide Versus Abiraterone as a First-Line Endocrine Therapy for Castration-
725 Resistant Prostate Cancer: Protocol for a Multicenter Randomized Phase 3 Trial. *JMIR*
726 *Res Protoc.* 7(7), e11191 (2018).
727

728

729 **Figure Legends**

730 **Figure 1. Within patient differential methylation analysis strategy to monitor temporal**
731 **changes in cfDNA.**

732 In order to help identify methylation changes associated with treatment in cfDNA, we opted to
733 perform within-patient methylation analysis to identify differentially methylated regions (DMRs)
734 associated with tumor response and/or resistance to current treatments. Each patient in this study
735 received either Enzalutamide or Abiraterone acetate and blood was collected prior to initiating
736 therapy (**Visit A**), at 12-weeks during treatment (**Visit B**) and upon clinical
737 progression/treatment change (**Visit C**). We applied an established genome-wide method to
738 detect methylated cfDNA fragments followed by extensive analysis to identify DMRs associated
739 with treatment response. We compared all study visits available (Visit B vs A, C vs B, and C vs
740 A) to find losses or gains in methylated cfDNA fragments. For instance, loss of treatment
741 responsive tumor cells (green methylated DNA fragments at visit B) or gains in treatment
742 insensitive/resistant tumor cells (blue DNA fragments at visit C) could be detected with this
743 strategy.

744

745 **Figure 2. Sample collection and patient clinical follow-up overview.**

746 (**a**) Plasma samples from mCRPC patients receiving Enzalutamide (12 patients) or Abiraterone
747 acetate (4 patients) were collected at baseline (Visit A), at week-12 (+/- 2 weeks, Visit B) and
748 upon clinical progression (Visit C). The total number of samples collected at each visit is shown.
749 2 Enzalutamide-treated patients (P2 and P26) were unable to provide samples for Visit C and 1
750 Abiraterone-treated patient (P36) progressed prior to Visit B. For these patients, the date of
751 treatment change/clinical progression was recorded for data analysis. (**b**) Pie chart summarizes

752 the distribution of metastasis locations at mCRPC diagnosis. (**c**) Bar plot shows best PSA
753 response for each patient during treatment (nadir), expressed as a percentage of Baseline/Visit A
754 PSA. Dotted line indicates ≥ 50% decline in PSA from Visit A. (**d**) Overall timeline of study
755 follow-up starting from Visit A to Visit C/Final visit is shown for all patients. Green dots
756 represent Visit B, red dots are Visit C or final study visit (if Visit C was not collected), yellow
757 indicates lowest PSA level (nadir) and blue dots show first PSA rise during treatment.
758
759 **Figure 3. Summary of intra-patient DMR analysis.**
760 (**a**) The total number of DMRs for all patients, visit comparison and treatment. (**b**) Boxplot
761 summarizing median, first and third quartile of all comparison DMRs. Whiskers represent the
762 highest and lowest number of DMRs. (**c**) DMR totals were further stratified by treatment type.
763 Boxplots illustrate percentage of DMRs that increased or decreased in methylation in (**d**) B vs A,
764 (**e**) C vs B and (**f**) C vs A. (**g**) The overall proportion of DMRs that were identified near/within
765 CGI, shore, TSS/promoter, ncRNA, intergenic and gene body regions is shown for all visit
766 comparisons (In order of B vs A, C vs B and C vs A). (**h**) Venn diagrams showing the overlap of
767 protein coding genes with DMRs near their promoters is shown for all visit comparisons and
768 between Enzalutamide- and Abiraterone-treated patients. (**i**) Similarly, the overlap of protein
769 coding regions with DMRs within gene bodies is shown.
770
771 **Figure 4. Key prostate cancer related methylation changes observed in cfDNA**
772 (**a**) Heatmap shows methylation trends in promoter regions for all patients and comparisons of
773 the most frequently methylated genes in PCa. For each gene, the proportion of DMRs with
774 increased (blue) and decreased (red) methylation was calculated and the net change is shown.

775 Grey indicates no net change in methylation. Representative peaks show methylation levels
776 (normalized read counts) of (**b**) *GSTP1* (black dotted lines indicating gene body) and (**c**) *TBX15*.
777 LNCaP cell line MeDIP-seq data is also shown.
778
779 **Figure 5. Common differentially methylated CpGs (DMCs).**
780 (**a**) For patients that were able to provide samples for all three visits, the proportion of CpG sites
781 that were differentially methylated in a single comparison and shared across 2 or more
782 comparisons is shown. 14 possible scenarios are represented by different colors. TTP in weeks
783 are also indicated for each patient. (**b**) Spearman correlation analysis of the proportion of DMCs
784 that were found to increase or decrease in B/C vs A (scenarios 9 & 10) against time to
785 progression (Spearman rho and p values are shown).
786
787 **Figure 6. NE-CRPC related DMRs in cfDNA.**
788 (**a**) For each patient, the proportion of DMRs that demonstrated methylation differences in NE-
789 CRPC associated regions in visit A vs B. (**b**) For DMRs that contained NE-CRPC associated
790 CpGs, various FDR thresholds were applied to assess for optimal regions that correlated with
791 TTP. (**c**) Using the optimal FDR cut-off, the ratio of NE-associated DMRs with increased
792 methylated fragments in visit A vs B to decreased fragments was correlated with TTP (Spearman
793 rho and p value is shown). For P36, A vs C comparison was used as this patient progressed prior
794 to visit B. (d) ROC analysis shows optimal AUC (0.927, 95% CI: 0.773-1) that stratifies patients
795 according to TTP (<25 weeks).

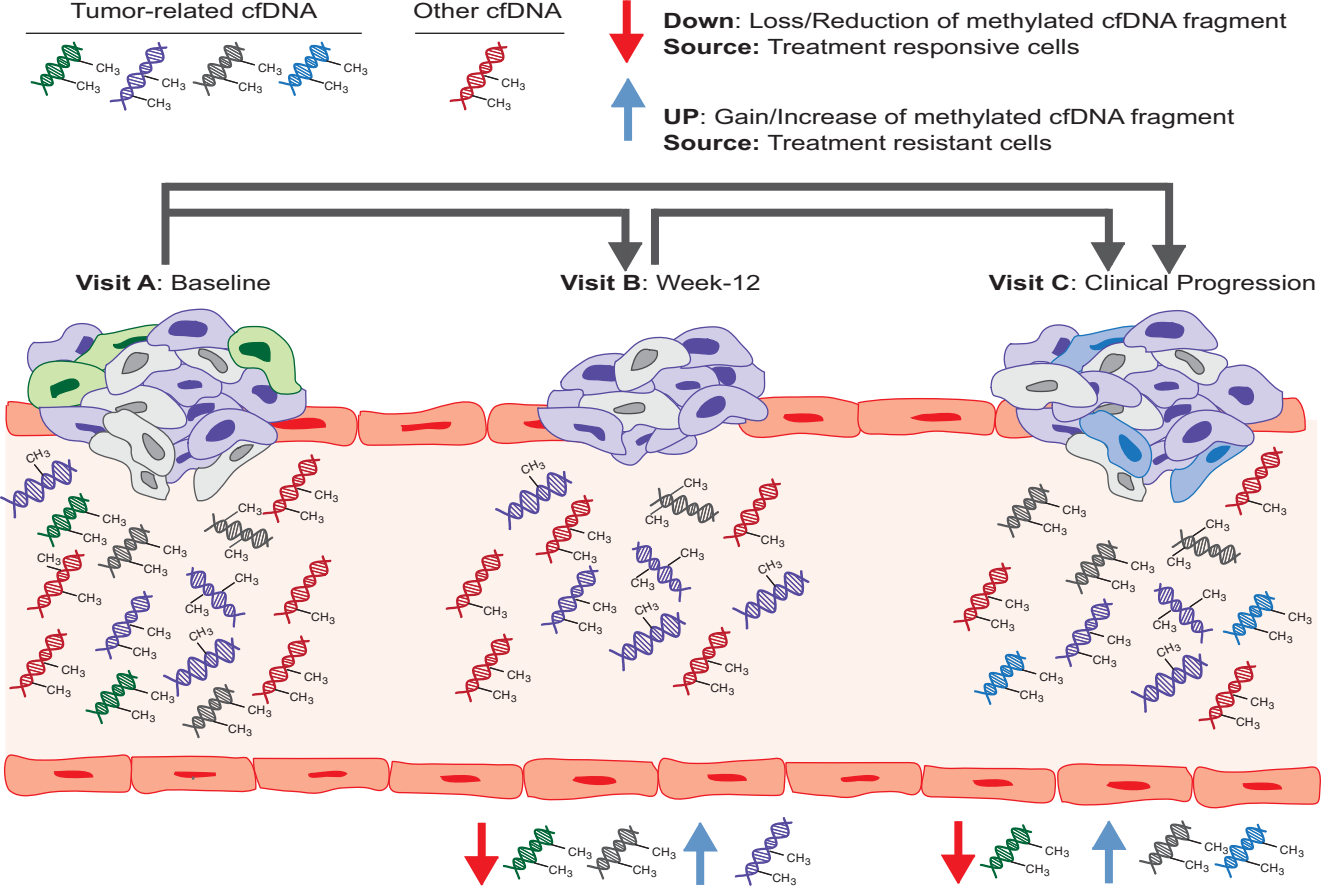
Tumor-related cfDNA
Other cfDNA
Down: Loss/Reduction of methylated cfDNA fragment
Source: Treatment responsive cells
UP: Gain/Increase of methylated cfDNA fragment
Source: Treatment resistant cells
Visit A: Baseline
Visit B: Week-12
Visit C: Clinical Progression

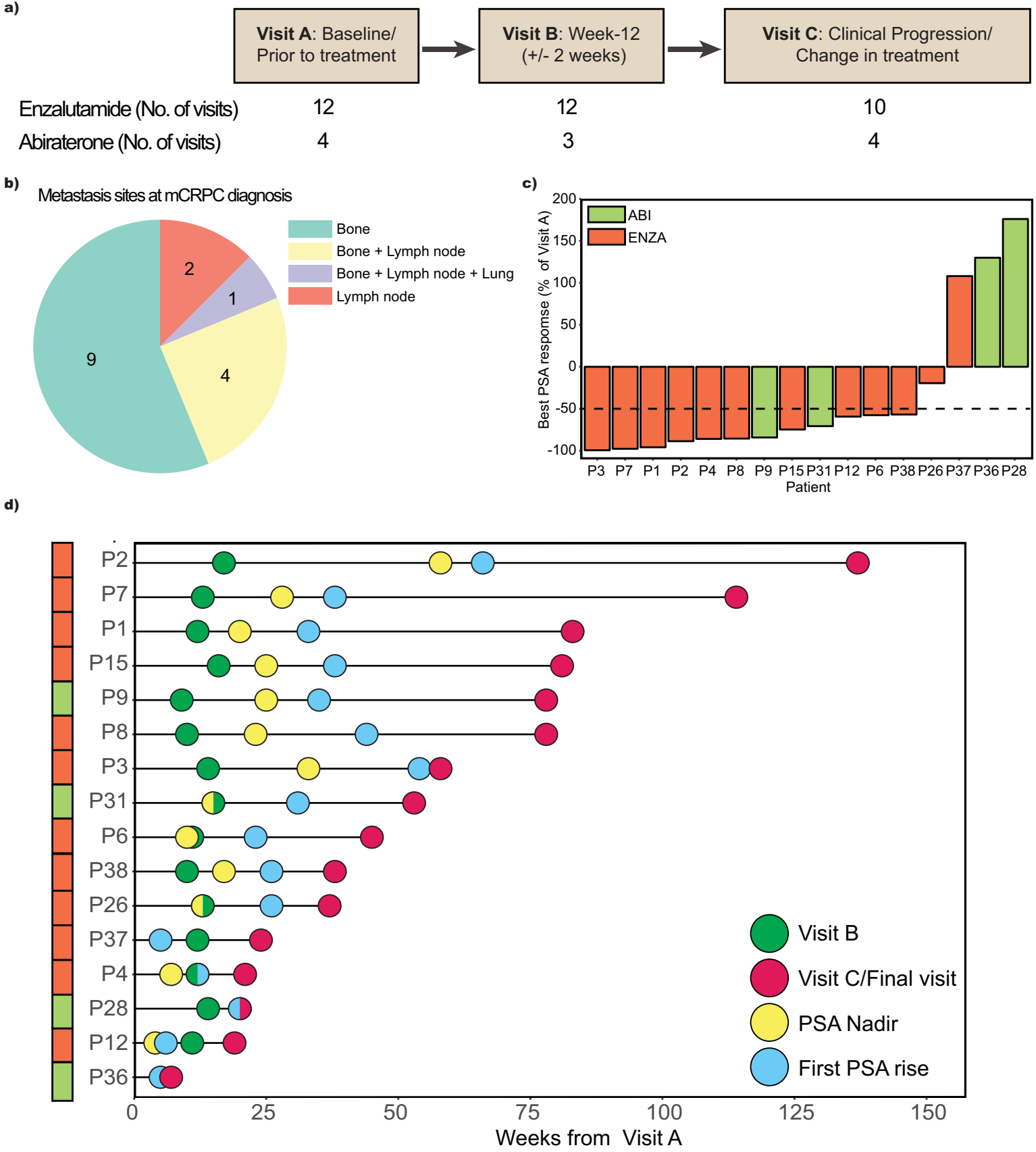
a)
Visit A: Baseline/ Prior to treatment
Visit B: Week-12 (+/- 2 weeks)
Visit C: Clinical Progression/ Change in treatment
Enzalutamide (No. of visits) 12 12 10
Abiraterone (No. of visits) 4 3 4
b)
Metastasis sites at mCRPC diagnosis
Bone
Bone + Lymph node
Bone + Lymph node + Lung
Lymph node
9
4
1
2
c)
ABI
ENZA
Best PSA response (% of Visit A)
200
150
100
50
0
-50
-100
P3 P7 P1 P2 P4 P8 P9 P15 P31 P12 P6 P38 P26 P37 P36 P28
Patient
d)
P2
P7
P1
P15
P9
P8
P3
P31
P6
P38
P26
P37
P4
P28
P12
P36
0 25 50 75 100 125 150
Weeks from Visit A
Visit B
Visit C/Final visit
PSA Nadir
First PSA rise

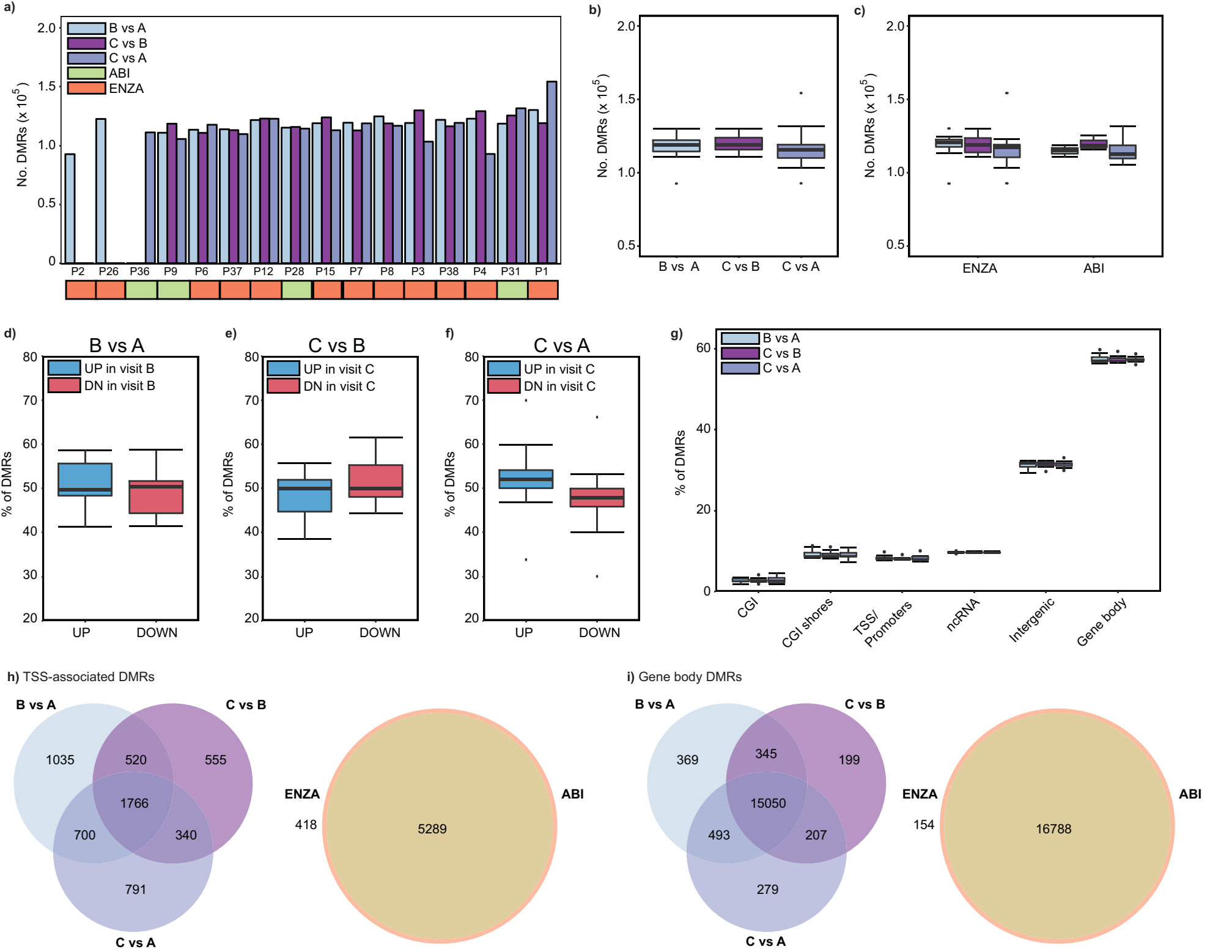
a)
B vs A
C vs B
C vs A
ABI
ENZA
No. DMRs (x 10^5)
P2 P26 P36 P9 P6 P37 P12 P28 P15 P7 P8 P3 P38 P4 P31 P1
b)
No. DMRs (x 10^5)
B vs A
C vs B
C vs A
c)
No. DMRs (x 10^5)
ENZA
ABI
d)
B vs A
UP in visit B
DN in visit B
% of DMRs
UP
DOWN
e)
C vs B
UP in visit C
DN in visit C
% of DMRs
UP
DOWN
f)
C vs A
UP in visit C
DN in visit C
% of DMRs
UP
DOWN
g)
B vs A
C vs B
C vs A
% of DMRs
CGI
CGI shores
TSS/ Promoters
ncRNA
Intergenic
Gene body
h) TSS-associated DMRs
B vs A
C vs B
C vs A
1035
520
555
1766
700
340
791
ENZA
ABI
418
5289
i) Gene body DMRs
B vs A
C vs B
C vs A
369
345
199
15050
493
207
279
ENZA
ABI
154
16788

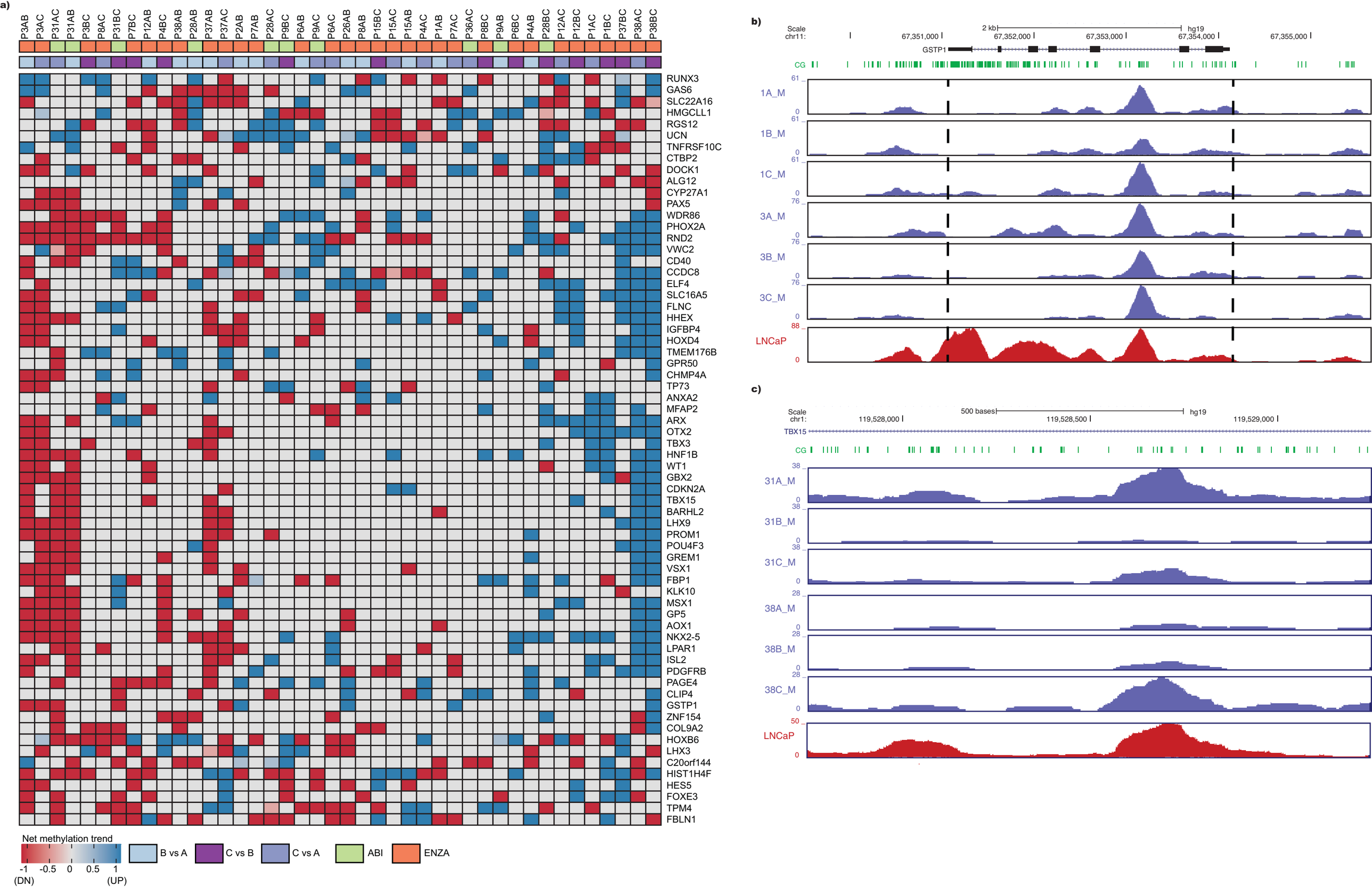
a)
P3AB P3AC P31AC P31AB P3BC P8AC P31BC P7BC P12AB P4BC P38AB P28AB P37AB P37AC P2AB P7AB P28AC P9BC P6AB P9AC P6AC P26AB P8AB P15BC P15AC P15AB P4AC P1AB P7AC P36AC P8BC P9AB P6BC P4AB P28BC P12AC P12BC P1AC P1BC P37BC P38AC P38BC
RUNX3
GAS6
SLC22A16
HMGCLL1
RGS12
UCN
TNFRSF10C
CTBP2
DOCK1
ALG12
CYP27A1
PAX5
WDR86
PHOX2A
RND2
VWC2
CD40
CCDC8
ELF4
SLC16A5
FLNC
HHEX
IGFBP4
HOXD4
TMEM176B
GPR50
CHMP4A
TP73
ANXA2
MFAP2
ARX
OTX2
TBX3
HNF1B
WT1
GBX2
CDKN2A
TBX15
BARHL2
LHX9
PROM1
POU4F3
GREM1
VSX1
FBP1
KLK10
MSX1
GP5
AOX1
NKX2-5
LPAR1
ISL2
PDGFRB
PAGE4
CLIP4
GSTP1
ZNF154
COL9A2
HOXB6
LHX3
C20orf144
HIST1H4F
HES5
FOXE3
TPM4
FBLN1
Net methylation trend
-1 -0.5 0 0.5 1
(DN) (UP)
B vs A
C vs B
C vs A
ABI
ENZA
b)
Scale
chr11:
67,351,000
2 kb
67,352,000
67,353,000
67,354,000
hg19
67,355,000
GSTP1
CG
1A_M
1B_M
1C_M
3A_M
3B_M
3C_M
LNCaP
c)
Scale
chr1:
119,528,000
500 bases
119,528,500
hg19
119,529,000
TBX15
CG
31A_M
31B_M
31C_M
38A_M
38B_M
38C_M
LNCaP

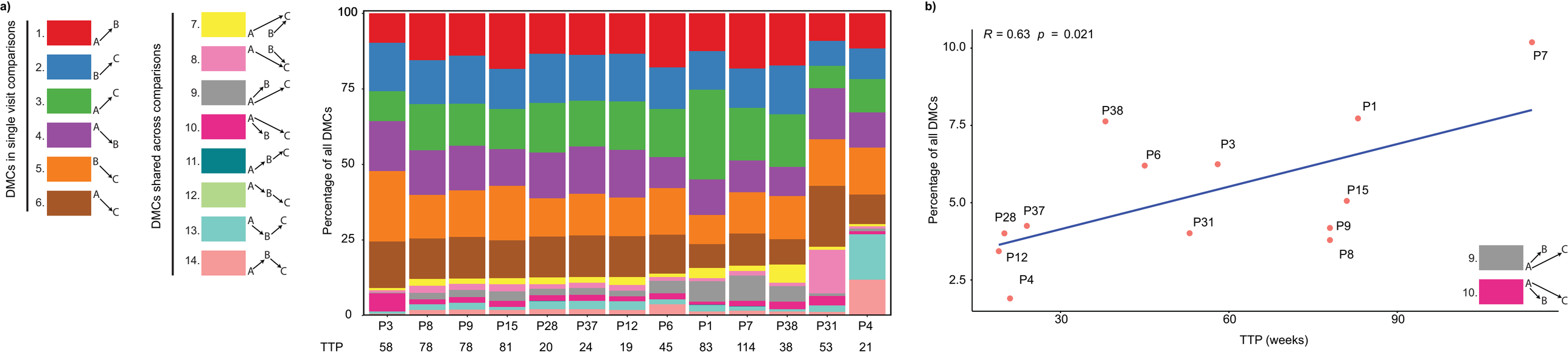
a)
DMCs in single visit comparisons
1. A→B
2. B→C
3. A→C
4. A→B
5. B→C
6. A→C
DMCs shared across comparisons
7. A→C, B→C
8. A→B, A→C
9. B→C, A→C
10. A→B, A→C
11. B→C, A→C
12. A→B→C
13. A→B→C
14. B→C, A→C
Percentage of all DMCs
100
75
50
25
0
P3 P8 P9 P15 P28 P37 P12 P6 P1 P7 P38 P31 P4
TTP 58 78 78 81 20 24 19 45 83 114 38 53 21
b)
R = 0.63 p = 0.021
Percentage of all DMCs
10.0
7.5
5.0
2.5
P7
P38
P1
P6
P3
P15
P28
P37
P31
P9
P12
P8
P4
30
60
90
TTP (weeks)
9. A→B→C
10. A→B→C

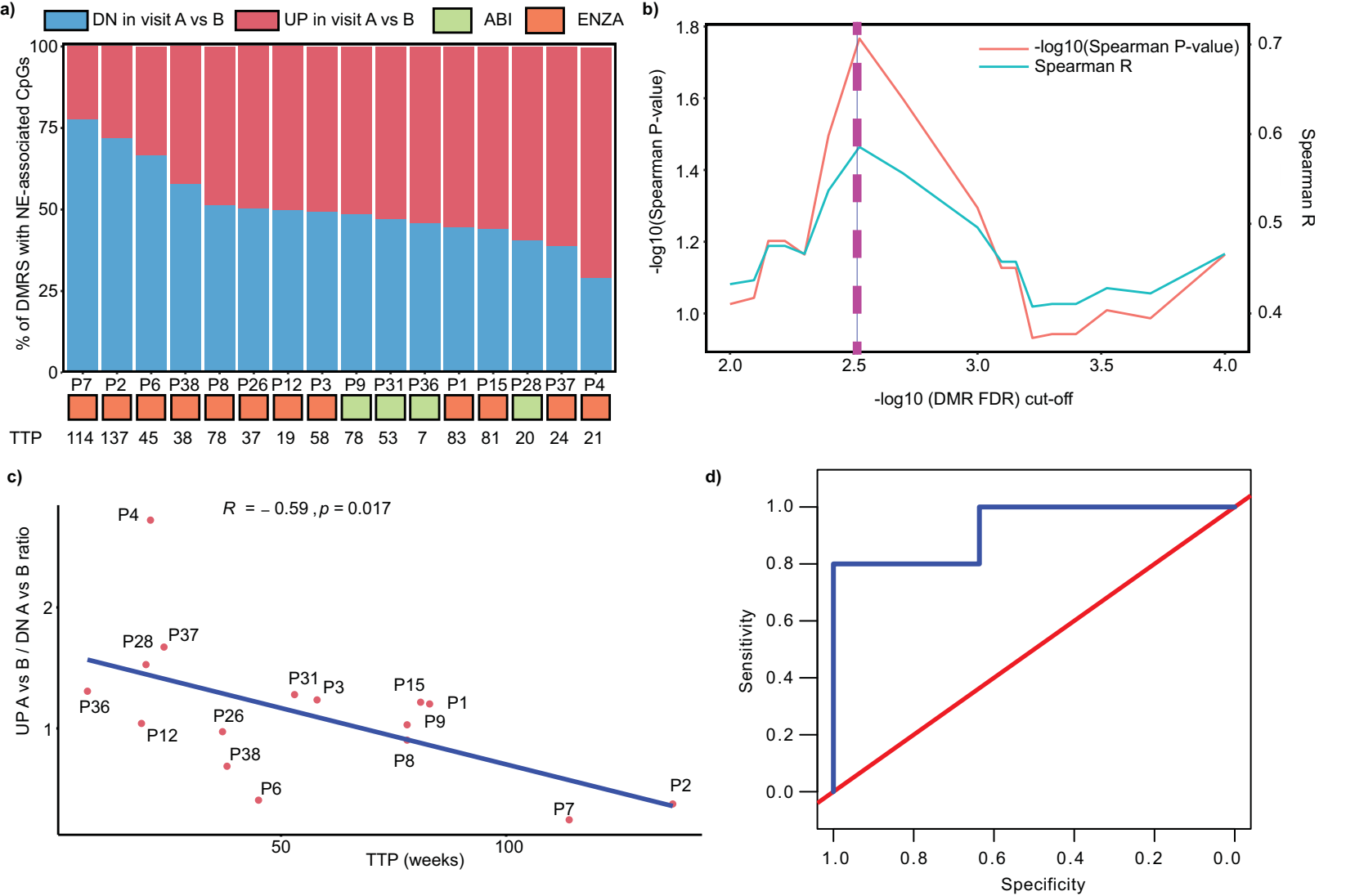
a)
DN in visit A vs B
UP in visit A vs B
ABI
ENZA
% of DMRS with NE-associated CpGs
100
75
50
25
0
P7 P2 P6 P38 P8 P26 P12 P3 P9 P31 P36 P1 P15 P28 P37 P4
TTP 114 137 45 38 78 37 19 58 78 53 7 83 81 20 24 21
b)
-log10(Spearman P-value)
Spearman R
1.8
1.6
1.4
1.2
1.0
0.7
0.6
0.5
0.4
2.0
2.5
3.0
3.5
4.0
-log10 (DMR FDR) cut-off
c)
R = – 0.59 , p = 0.017
UP A vs B / DN A vs B ratio
2
1
P4
P28
P37
P36
P12
P26
P38
P6
P31
P3
P15
P1
P9
P8
P7
P2
50
100
TTP (weeks)
d)
Sensitivity
1.0
0.8
0.6
0.4
0.2
0.0
Specificity